Available online at www.sciencedirect.com
SCIENCE DIRECT®
Journal of Magnetic Resonance 171 (2004) 193–200
JMR Journal of Magnetic Resonance
www.elsevier.com/locate/jmr

Random coil phosphorus chemical shift of deoxyribonucleic acids

Cheuk Nang Ho, Sik Lok Lam*

Department of Chemistry, The Chinese University of Hong Kong, Shatin, New Territories, Hong Kong

Received 14 July 2004; revised 27 August 2004
Available online 22 September 2004

Abstract

Random coil phosphorus chemical shift has been studied using 16 17-nucleotide DNA sequences. Due to the presence of residual base stacking in these sequences, the temperature and sequence effects were investigated at 50 and 55 °C. The phosphorus chemical shifts of random coil DNA sequences have been found to be independent of temperature. Sequence effect analysis shows that the phosphorus chemical shift of a nucleotide in a random coil DNA sequence depends on both its 5′- and 3′-nearest neighbors. A trimer model has been used to establish the random coil ^{31}P chemical shift prediction protocol which shows an accuracy of 0.02 ppm.

Keywords: Phosphorus chemical shift; DNA; Random coil; Sequence effect

1. Introduction

Solution structure of deoxyribonucleic acid (DNA) is conventionally determined by refining a model structure with a set of nuclear magnetic resonance (NMR) structural constraints including nuclear overhauser effect (NOE) derived distances and scalar coupling derived torsion angles [1]. Due to the severe spectral overlapping of the DNA backbone H4′, H5′, and H5″ protons, their chemical shift assignments are usually ambiguous. This limits the number of structural constraints derived from these protons, leading to a difficulty in determining the backbone conformation. NMR spectroscopic studies have shown that phosphorus (^{31}P) chemical shift contains wealthy information about the DNA backbone conformation [2–12]. Therefore, ^{31}P chemical shift is potentially useful in determining solution DNA structures.

To make use of ^{31}P chemical shift, it is necessary to investigate and establish the structure and ^{31}P chemical shift relationship. For B-form DNA duplexes, quantum mechanical calculations have shown that the backbone ^{31}P chemical shift depends mainly on the conformations of two of the six backbone torsion angles, namely, α (O3′–P–O5′–C5′) and ζ (C3′–O3′–P–O5′) (Fig. 1) [6,13,14]. Apart from the dependence on these torsion angles, the backbone ^{31}P chemical shift is also influenced by other factors such as bond angles [6,15,16], neighboring nucleotides [8,17], counter-ions [17], solvents [12,17–19], and temperature [4,5,20]. For random coil DNA sequences in which no intra- or inter-strand hydrogen bonds and base stacking are present, their ^{31}P chemical shifts have been found to be more downfield from those of single, double, and triple helices [4,10]. Not much work has been done to define the chemical shifts of random coil DNA sequences because these shifts are sequence dependent and the measurement with low molecular weight model compounds may strongly be influenced by intermolecular interactions [21]. Recently, random coil DNA proton [22] and carbon [23] chemical shifts have been studied successfully by using 16 17-nucleotide DNA sequences prepared in 8 M urea solution. To complement the random coil DNA chemical shift information and to further examine the use of ^{31}P chemical shift in defining DNA backbone structures, the present study aims to determine the temperature and sequence effects on ran-

* Corresponding author. Fax: +852 2603 5057.
E-mail address: lams@cuhk.edu.hk (S.L. Lam).

1090-7807/$ - see front matter
doi:10.1016/j.jmr.2004.08.024

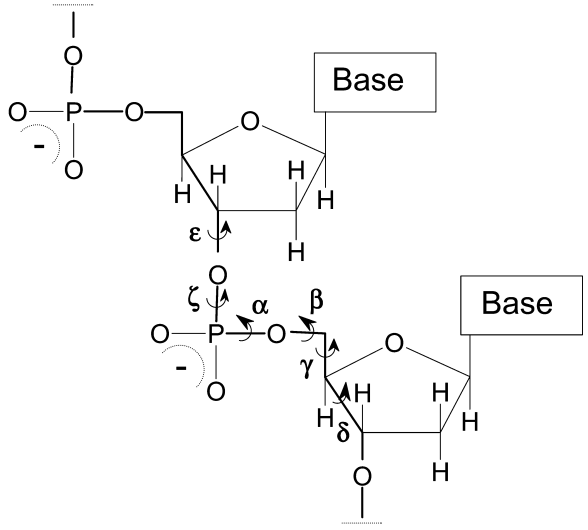

Fig. 1. Definitions of DNA backbone torsion angles.

dom coil DNA ^{31}P chemical shift. Based on sequence effect analysis, a random coil ^{31}P chemical shift prediction protocol has been developed, allowing the prediction of the ^{31}P chemical shift of a nucleotide in any random coil sequences.

2. Experimental

2.1. DNA samples

Sixteen 17-nucleotide DNA sequences (namely SS1–SS16 as shown in Table 1), which had been used to study random coil proton [22] and carbon chemical shifts [23], were employed in this study to investigate the temperature and sequence effects on random coil ^{31}P chemical shift. Ten additional sequences including four 17-nucleotide, four 15-nucleotide, and two 11-nucleotide were also prepared for testing the accuracy of the random coil DNA ^{31}P chemical shift prediction protocol. All these sequences were synthesized using solid-phase phosphoramidite chemistry in an Applied Biosystems Model 392 DNA synthesizer and purified by polyacrylamide gel electrophoresis. NMR samples were prepared by making a 1.0 mM DNA in 500 μl solution containing 8 M urea, 0.1 mM of 2,2-dimethyl-2-silapentane-5-sulfonic acid (DSS), 150 mM sodium chloride, and 10 mM sodium phosphate at pH 7. The samples were dried, re-dissovled in 99.9% D_2O twice, and finally put into 5 mm Wilmad PP528 NMR tubes.

2.2. NMR measurements

All NMR experiments were performed on a Bruker ARX-500 NMR spectrometer operating at 500.13 MHz for proton. A 5 mm inverse broadband probe was used and the acquired spectral data were processed using Bruker XWIN-NMR software. The most upfield signal of DSS was set at 0 ppm to serve as an internal chemical shift reference. For the ^{31}P resonance assignments of SS1–SS16, ^{1}H–^{31}P HSQC experiments were performed at 25 °C using the TPPI method [24] with the exception that the experiments for SS7 and SS16 were run at 35 °C to remove the residual structures [22]. A 4k × 256 dataset was acquired for each spectrum. The ^{1}H spectral width was set to 11 ppm with the carrier frequency positioned at the residual HDO signal. The ^{31}P spectral width was set to 1 ppm and heteronuclear decoupling was executed by WALTZ-16 composite pulse decoupling

Table 1
DNA sequences used in studying the sequence effect on random coil DNA chemical shifts[a]

Sequence name	Nucleotide position																
	1	2	3	4	5	6	7	8	9	10	11	12	13	14	15	16	17
SS1	**T**	C	C	C	**T**	T	A	G	**T**	A	G	A	**T**	G	C	T	**T**
SS2	**T**	G	C	C	**T**	C	T	G	**T**	T	G	A	**T**	A	C	T	**T**
SS3	**T**	A	C	C	**T**	G	T	G	**T**	C	A	A	**T**	T	C	T	**T**
SS4	**T**	T	C	C	**T**	A	T	G	**T**	G	A	A	**T**	C	G	T	**T**
SS5	**T**	C	G	C	**T**	T	T	G	**T**	A	A	A	**T**	G	G	T	**T**
SS6	**T**	G	G	C	**T**	C	C	G	**T**	T	A	A	**T**	A	G	T	**T**
SS7	**T**	A	G	C	**T**	G	C	G	T	C	T	A	**T**	T	G	T	**T**
SS8	**T**	T	G	C	**T**	A	C	G	**T**	G	T	A	**T**	C	A	T	**T**
SS9	**T**	C	A	C	**T**	T	C	G	**T**	A	T	A	**T**	G	A	T	**T**
SS10	**T**	G	A	C	**T**	C	G	G	**T**	T	T	A	T	A	A	T	**T**
SS11	**T**	A	A	C	**T**	G	G	G	T	C	C	A	**T**	T	A	T	**T**
SS12	**T**	T	A	C	**T**	A	G	G	**T**	G	C	A	**T**	C	T	T	**T**
SS13	**T**	C	T	C	**T**	T	G	G	**T**	A	C	A	**T**	G	T	T	**T**
SS14	**T**	G	T	C	**T**	C	A	G	**T**	T	C	A	**T**	A	T	T	**T**
SS15	**T**	A	T	C	**T**	G	A	G	**T**	C	G	A	**T**	T	T	T	**T**
SS16	**T**	T	T	C	**T**	A	A	G	**T**	G	G	A	**T**	C	C	T	**T**

[a] Each sequence contains four different types of triplets separated by thymine nucleotides. All 64 different types of triplets are included.

sequence [25–27]. Zero-filling and baseline corrections were applied to generate a 1k × 1k data matrix. ^{31}P chemical shifts were indirectly referenced to DSS using the derived nucleus-specific ratio (Ξ) of 0.404808636 [28]. ^{1}H–^{31}P HSQC experiments were repeated at 50 and 55 °C to determine the temperature effect on random coil ^{31}P chemical shift. Ambiguous ^{31}P assignments were resolved by performing ^{1}H–^{31}P HSQC–TOCSY experiments [29] in which a DIPSI-2 composite pulse sequence [30] was used in the isotropic mixing period. The experimental parameters were set as the same as in HSQC experiments except the ^{31}P spectral width was set to 3 ppm.

3. Results and discussion

Based on the H3′ assignments of SS1–SS16 [22], the ^{31}P resonance signals were assigned using the ^{1}H–^{31}P HSQC spectra. The ^{31}P assignments of some residues were found to be ambiguous due to their H3′ protons having the same chemical shifts. Under these circumstances, the more well-resolved H1′ regions of the HSQC–TOCSY spectra become useful for assigning the ^{31}P signals. Fig. 2 shows the $H1'_{i-1}$–P_i and $H3'_{i-1}$–P_i (where i indicates the ith residue) regions of the HSQC–TOCSY spectrum of SS1. The ^{31}P chemical shift assignments of A10p and G11p (the "p" indicates the phosphorus is attached to the 3′-end of the residue) were obtained from the unambiguous assignment of the H1′ chemical shifts of A10 and G11. With the help of the HSQC–TOCSY spectra, all ^{31}P chemical shifts of SS1–SS16 were successfully assigned and the results are summarized in the supplementary materials.

3.1. Temperature effect

To study the temperature effect, the ^{31}P chemical shifts of SS1–SS16 were also measured at 50 and 55 °C (supplementary materials). In general, the changes in the ^{31}P chemical shifts of most residues over a 25 °C change in temperature were found to be quite small. These changes are of the same order of magnitude as the ^{31}P chemical shift measurement uncertainty (0.01 ppm), indicating the temperature effect is negligibly small. However, the changes of some residues were found to be a bit large (up to ∼0.1 ppm). Such changes are probably due to the presence of a small extent of residual base stacking at room temperature because ^{31}P chemical shift has been shown to be sensitive to base stacking and base stacking has been found to exist in single-strand DNA sequences [11]. The term "residual" was suggested here because the observed chemical shift changes were only up to ∼0.1 ppm, instead of ∼1 ppm for the removal of strong base stacking in single-strand helices.

To verify the changes in ^{31}P chemical shifts are due to residual base stacking but not temperature, these changes were re-analyzed in terms of dimers because residual base stacking is expected to occur preferentially in purine–purine dimers [11]. For each type of dimers, a total of eight chemical shift values were obtained at each temperature. For example, two values were obtained from SS1 for the CC dimer and the other six were from SS2, SS3, SS4, SS6, SS11, and SS16, respectively. These values were then used to calculate the average temperature coefficients in two different temperature ranges: 25–50 and 50–55 °C. In Table 2, the temperature coefficients for most dimers in the 25–50 °C temperature range reveal the ^{31}P chemical shift changes over a 10 °C change

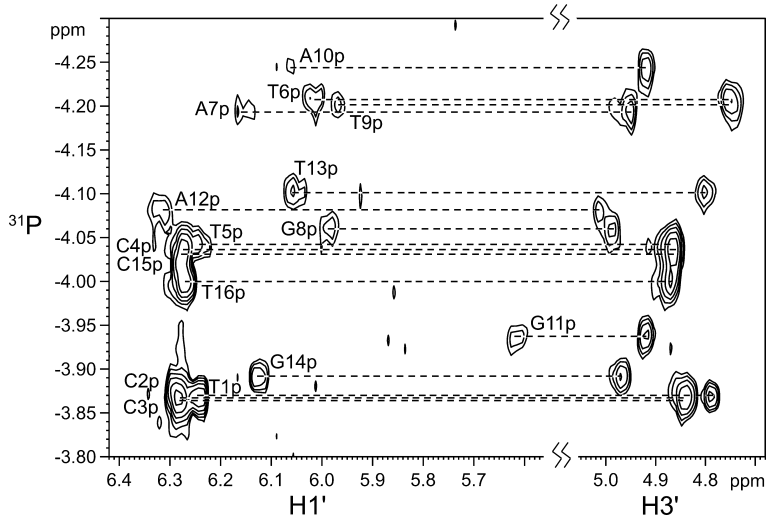

Fig. 2. The H1′ and H3′ regions of the HSQC–TOCSY spectrum of SS1.

Table 2
Average ^{31}P chemical shift temperature coefficients of different types of dimers

Dimer	Temperature coefficients (ppm/10 °C)[a]	
	Between 25 and 50 °C	Between 50 and 55 °C
Pyrimidine–pyrimidine		
CT	0.01 (0.00)	0.01 (0.01)
CC	0.00 (0.00)	0.00 (0.01)
TC	0.00 (0.00)	0.01 (0.01)
TT	0.01 (0.00)	0.01 (0.01)
Pyrimidine–purine		
CA	0.01 (0.00)	0.00 (0.01)
CG	0.01 (0.00)	0.01 (0.01)
TA	0.01 (0.01)	0.01 (0.01)
TG	0.02 (0.01)	0.00 (0.01)
Purine–pyrimidine		
AC	0.01 (0.01)	0.01 (0.01)
AT	0.02 (0.00)	0.01 (0.01)
GC	0.00 (0.00)	0.01 (0.01)
GT	0.01 (0.01)	0.01 (0.01)
Purine–purine		
AA	0.02 (0.01)	0.00 (0.01)
AG	0.03 (0.01)	0.00 (0.01)
GA	−0.01 (0.01)	0.01 (0.01)
GG	0.02 (0.01)	0.01 (0.01)

[a] The values in parentheses represent the standard deviations of the averaged values.

in temperature are close to or smaller than the chemical shift measurement uncertainty. A few dimers including pyrimidine–purine TG, purine–pyrimidine AT, and purine–purine AA and GG possess a temperature coefficient of 0.02 ppm/10 °C. The largest one belongs to the purine–purine dimer, AG, which possesses a temperature coefficient of 0.03 ppm/10 °C. Due to the decomposition of urea at higher temperatures, ^{31}P chemical shifts were measured up to 55 °C. Although chemical shift measurement at a higher temperature gives a more accurate temperature coefficient, a temperature range of 5 °C is enough for determining a temperature coefficient of 0.03 ppm/10 °C. In the 50–55 °C range, all temperature coefficients including the one for the AG dimer were found to be less than or equal to 0.01 ppm/10 °C, indicating no residual base stacking is present at or above 50 °C and the temperature effect is indeed insignificant. Therefore, the chemical shifts measured at 50 °C were used to study the sequence effect on random coil DNA ^{31}P chemical shift.

3.2. Sequence effect

Based on the chemical shift assignment at 50 °C, the sequence effect on random coil DNA ^{31}P chemical shifts were then determined. This effect includes the 5′- and 3′-nearest neighbor effects and the 5′-next nearest neighbor effect. The significance of the 5′-nearest neighbor effects ($\Delta_1^{5'}$) was investigated by comparing the T16 ^{31}P chemical shift. In Table 3, SS1–SS16 sequences are arranged into four groups such that nucleotides 12–17 (except nucleotide 15, which is the 5′-nearest neighbor of T16) in each group are the same. The T16 chemical shift with

Table 3
5′-nearest neighbor effect on random coil DNA ^{31}P chemical shift

Sequence name	Nucleotide position						$\Delta_1^{5'}$(ppm)[b]
	12	13	14	15[a]	16	17	
Group A							
SS16	A	T	C	**C**	T (−4.02)	T	0.05
SS4	A	T	C	**G**	T (−4.05)	T	0.02
SS8	A	T	C	**A**	T (−4.07)	T	0.00
SS12	A	T	C	**T**	T (−4.04)	T	0.03
Group B							
SS1	A	T	G	**C**	T (−4.03)	T	0.03
SS5	A	T	G	**G**	T (−4.05)	T	0.01
SS9	A	T	G	**A**	T (−4.06)	T	0.00
SS13	A	T	G	**T**	T (−4.02)	T	0.04
Group C							
SS2	A	T	A	**C**	T (−4.01)	T	0.05
SS6	A	T	A	**G**	T (−4.05)	T	0.01
SS10	A	T	A	**A**	T (−4.06)	T	0.00
SS14	A	T	A	**T**	T (−4.04)	T	0.02
Group D							
SS3	A	T	T	**C**	T (−4.02)	T	0.06
SS7	A	T	T	**G**	T (−4.05)	T	0.03
SS11	A	T	T	**A**	T (−4.08)	T	0.00
SS15	A	T	T	**T**	T (−4.04)	T	0.04

[a] The bolded nucleotides at position 15 are the 5′-nearest neighbors of T16.
[b] $\Delta_1^{5'}$ represents the 5′-nearest neighbor effect on T16. $\Delta_1^{5'} = \delta_{T16} - \delta_{T16A}$, where δ_{T16} is the T16 chemical shift and δ_{T16A} is the T16 chemical shift with an adenine nucleotide as the 5′-nearest neighbor in the group.

an adenine nucleotide as the 5′-nearest neighbor (δ_{T16A}) in each group (usually the most upfield shift) was subtracted from the T16 chemical shift (δ_{T16}) of each sequence. The significance of the 5′-nearest neighbor effect ($\Delta_1^{5'}$) is defined by the chemical shift difference (δ_{T16}–δ_{T16A}), which shows the effect of substituting the 5′-nearest adenine nucleotide with a different nucleotide. The largest $\Delta_1^{5'}$ value was found to be 0.06 ppm, indicating the ^{31}P chemical shift of a nucleotide in a random coil DNA sequence depends on its 5′-nearest neighbor.

Similarly, the significance of the 3′-nearest neighbor effect ($\Delta_1^{3'}$) was investigated by comparing the ^{31}P chemical shifts of nucleotide 2 (X2) of the 16 DNA sequences. In Table 4, the sequences are arranged such that nucleotides 1–5 (except nucleotide 3, which is the 3′-nearest neighbor of X2) in each group are the same. The chemical shift of X2 with an adenine nucleotide as the 3′-nearest neighbor (δ_{X2A}) in each group was subtracted from the X2 chemical shift (δ_{X2}) of each sequence. The chemical shift difference ($\delta_{X2} - \delta_{X2A}$) indicates the significance of the 3′-nearest neighbor effect. In most cases, the $\Delta_1^{3'}$ values were found to be negligibly small. The 3′-nearest neighbor effect is obviously less significant than the 5′-nearest neighbor effect. However, when an adenine nucleotide was substituted by a thymine nucleotide, the $\Delta_1^{3'}$ value could be as large as 0.05 ppm, indicating the ^{31}P chemical shift of a nucleotide in a random coil DNA sequence also depends on its 3′-nearest neighbor.

For the 5′-next nearest neighbor effect ($\Delta_2^{5'}$), the ^{31}P chemical shifts of T16 of the 16 DNA sequences are compared in Table 5. Almost all $\Delta_2^{5'}$ values were determined to be close to or less than the measurement uncertainty, indicating the 5′-next nearest neighbor effect is negligibly small. As the backbone phosphate of a nucleotide in a random coil DNA sequence is located closer to its 5′-next nearest neighbor than its 3′-next nearest neighbor, this result also reveals the 3′-next nearest neighbor effect is negligibly small.

3.3. Prediction protocol

The above analysis on neighbor effects indicates that the random coil ^{31}P chemical shift of a specific nucleotide in a DNA sequence depends on both its 5′- and 3′-nearest neighbors. Based on the ^{31}P chemical shifts of SS1–SS16 at 50 °C, a trimer model random coil DNA ^{31}P chemical shift database has been established (Table 6). The ^{31}P chemical shifts of the 64 triplets ($N^{5'}pXN^{3'}$) in SS1–SS16 were used as the trimer values (δ_{trimer}). To predict the ^{31}P chemical shift of a specific nucleotide X with its 5′-nearest neighbor ($N^{5'}$) and 3′-nearest neighbor ($N^{3'}$) in a random coil DNA sequence, the δ_{trimer} value corresponding to $N^{5'}pXN^{3'}$ in the database is used. For example, the predicted random coil ^{31}P chemical shift of G4 in 5′-G1-T2-A3-**G4**-C5-T6-A7-G8-G9-T10-G11-3′ is equal to the δ_{trimer} value of the AGC trimer (−4.12 ppm) in Table 6. The experimental value

Table 4
3′-nearest neighbor effect on random coil DNA ^{31}P chemical shift

Sequence name	Nucleotide position					$\Delta_1^{3'}$ (ppm)[b]
	1	2	3[a]	4	5	
Group A						
SS1	T	C (−3.88)	**C**	C	T	−0.01
SS5	T	C (−3.88)	**G**	C	T	−0.01
SS9	T	C (−3.87)	**A**	C	T	0.00
SS13	T	C (−3.86)	**T**	C	T	0.01
Group B						
SS2	T	G (−4.01)	**C**	C	T	0.01
SS6	T	G (−4.01)	**G**	C	T	0.01
SS10	T	G (−4.02)	**A**	C	T	0.00
SS14	T	G (−3.98)	**T**	C	T	0.04
Group C						
SS3	T	A (−4.01)	**C**	C	T	0.02
SS7	T	A (−4.03)	**G**	C	T	0.00
SS11	T	A (−4.03)	**A**	C	T	0.00
SS15	T	A (−3.98)	**T**	C	T	0.05
Group D						
SS4	T	T (−3.99)	**C**	C	T	0.00
SS8	T	T (−3.99)	**G**	C	T	0.00
SS12	T	T (−3.99)	**A**	C	T	0.00
SS16	T	T (−3.97)	**T**	C	T	0.02

[a] The bolded nucleotides at position 3 are the 3′-nearest neighbors of nucleotide 2 (X2).
[b] $\Delta_1^{3'}$ represents the 3′-nearest neighbor effect on X2. $\Delta_1^{3'} = \delta_{X2} - \delta_{X2A}$, where δ_{X2} is the X2 chemical shift and δ_{X2A} is the X2 chemical shift with an adenine nucleotide as the 3′-nearest neighbor in the group.

Table 5
5′-next nearest neighbor effect on random coil DNA ^{31}P chemical shift

Sequence name	Nucleotide position						$\Delta_2^{5'}$ (ppm)[b]
	12	13	14[a]	15	16	17	
Group A							
SS16	A	T	**C**	C	T (−4.02)	T	−0.01
SS1	A	T	**G**	C	T (−4.03)	T	−0.02
SS2	A	T	**A**	C	T (−4.01)	T	0.00
SS3	A	T	**T**	C	T (−4.02)	T	−0.01
Group B							
SS4	A	T	**C**	G	T (−4.05)	T	0.00
SS5	A	T	**G**	G	T (−4.05)	T	0.00
SS6	A	T	**A**	G	T (−4.05)	T	0.00
SS7	A	T	**T**	G	T (−4.05)	T	0.00
Group C							
SS8	A	T	**C**	A	T (−4.07)	T	−0.01
SS9	A	T	**G**	A	T (−4.06)	T	0.00
SS10	A	T	**A**	A	T (−4.06)	T	0.00
SS11	A	T	**T**	A	T (−4.08)	T	−0.02
Group D							
SS12	A	T	**C**	T	T (−4.04)	T	0.00
SS13	A	T	**G**	T	T (−4.02)	T	0.02
SS14	A	T	**A**	T	T (−4.04)	T	0.00
SS15	A	T	**T**	T	T (−4.04)	T	0.00

[a] The bolded nucleotides at position 14 are the 5′-next nearest neighbors of T16.
[b] $\Delta_2^{5'}$ represents the 5′-next nearest neighbor effect on T16. $\Delta_2^{5'} = \delta_{T16} - \delta_{T16A}$, where δ_{T16} is the T16 chemical shift and δ_{T16A} is the T16 chemical shift with an adenine nucleotide as the 5′-next nearest neighbor in the group.

Table 6
Trimer model random coil ^{31}P chemical shift database[a]

$N^{5'}$ pCN$^{3'}$	δ_{trimer} (ppm)	$N^{5'}$ pGN$^{3'}$	δ_{trimer} (ppm)	$N^{5'}$ pAN$^{3'}$	δ_{trimer} (ppm)	$N^{5'}$ pTN$^{3'}$	δ_{trimer} (ppm)
CCC	−3.88	CGC	−3.98	CAC	−4.01	CTC	−4.00
GCC	−3.89	GGC	−4.01	GAC	−4.01	GTC	−4.05
ACC	−3.92	AGC	−4.12	AAC	−4.13	ATC	−4.06
TCC	−3.88	TGC	−4.04	TAC	−4.09	TTC	−4.02
CCG	−3.87	CGG	−3.99	CAG	−4.05	CTG	−3.99
GCG	−3.88	GGG	−4.05	GAG	−4.06	GTG	−4.02
ACG	−3.90	AGG	−4.14	AAG	−4.15	ATG	−4.03
TCG	−3.89	TGG	−4.08	TAG	−4.14	TTG	−4.01
CCA	−3.88	CGA	−4.00	CAA	−4.05	CTA	−3.99
GCA	−3.89	GGA	−4.06	GAA	−4.05	GTA	−4.04
ACA	−3.91	AGA	−4.15	AAA	−4.15	ATA	−4.04
TCA	−3.91	TGA	−4.07	TAA	−4.13	TTA	−4.01
CCT	−3.89	CGT	−3.97	CAT	−4.01	CTT	−4.00
GCT	−3.90	GGT	−4.03	GAT	−4.02	GTT	−4.03
ACT	−3.92	AGT	−4.12	AAT	−4.11	ATT	−4.05
TCT	−3.90	TGT	−4.05	TAT	−4.10	TTT	−4.03

[a] Uncertainty in ^{31}P chemical shift measurement was ± 0.01 ppm.

was found to be −4.13 ppm, which shows only a 0.01 ppm deviation from the predicted value.

To further test the prediction accuracy, a total of 280 random coil ^{31}P chemical shift values were used. These experimental values include 160 data from SS1 to SS16 that have not been used in establishing the trimer model database and 120 data from 10 new random coil DNA sequences containing 9–17 nucleotides. Fig. 3 shows a plot of the predicted values versus the experiment values. The root-mean-square deviation (RMSD) value between the predicted (δ_{pred}) and the experimental (δ_{expt}) values was found to be 0.02 ppm with a correlation coefficient of 0.970.

Although the 3′-nearest neighbor effect has been shown to be less significant in affecting random coil ^{31}P chemical shift than the 5′-nearest neighbor effect, ignoring the 3′-nearest neighbor effect in developing the prediction protocol probably decreases the prediction accuracy. An attempt has been made to develop a prediction protocol based on a dimer model (supple-

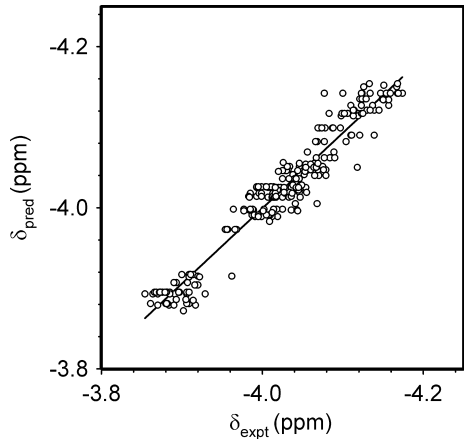

Fig. 3. A plot of the predicted random coil DNA ^{31}P chemical shifts versus the experimental shifts using the trimer model prediction protocol.

mentary materials). The RMSD between 216 predicted and experimental values was found to be 0.03 ppm with a correlation coefficient of 0.951, indicating that the trimer model prediction protocol is more reliable.

In the above ^{31}P chemical shift prediction analysis, all random coil ^{31}P chemical shift values from the second and the last nucleotides of the testing sequences have been neglected because they were influenced by end effects. Due to the absence of a phosphate group at both the 5′- and 3′-ends, the predicted values were usually found to be more upfield than the experimental values, indicating random coil ^{31}P chemical shift depends not only on sequence but also on the electrostatic contributions from neighboring phosphate groups. Based on 26 random coil ^{31}P chemical shift values from the second and the last nucleotides of the testing sequences, the 5′ and 3′-end effect correction shifts were calculated to be 0.05 and 0.06 ppm, respectively.

Apart from this newly developed prediction protocol on random coil ^{31}P chemical shift, the previously developed protocols on random coil proton [22] and carbon [23] chemical shifts were all based on the corrections of neighbor effects. As the only difference among the neighboring nucleotides is the type of the bases, this suggests the origin of the sequence effect is mainly due to the aromatic ring currents from the neighboring bases. The high prediction accuracy of these protocols indicates the ring current effect is responsible for the observed variations in chemical shifts of different random coil DNA sequences.

4. Conclusions

The temperature effect on random coil ^{31}P chemical shift has been found to be negligibly small. Sequence effect analysis shows that the ^{31}P chemical shift of a nucleotide in a random coil DNA sequence depends on both its 5′- and 3′-nearest neighbors. A trimer model random coil ^{31}P chemical shift prediction protocol has been developed and demonstrated to give accurate prediction results.

Acknowledgments

This research was partially supported by an anonymous donor who made the donation to the Department of Chemistry at The Chinese University of Hong Kong and a grant from the Research Grants Council of the Hong Kong Special Administrative Region, China (Project No. CUHK4047/02P).

Appendix. Supplementary material

Supplementary data associated with this article can be found, in the online version, at doi:10.1016/j.jmr.2004.08.024.

References

[1] S.S. Wijmenga, B.N.M. van Buuren, The use of NMR methods for conformational studies of nucleic acids, Prog. Nucl. Magn. Reson. Spectrosc. 32 (1998) 287–387.
[2] D.G. Gorenstein, ^{31}P NMR of DNA, Methods Enzymol. 211 (1992) 254–286.
[3] D.G. Gorenstein, Conformation and dynamics of DNA and protein-DNA complexes by ^{31}P NMR, Chem. Rev. 94 (1994) 1315–1338.
[4] D.G. Gorenstein, J.B. Findlay, R.K. Momii, B.A. Luxon, D. Kar, Temperature dependence of the ^{31}P chemical shifts of nucleic acids. A probe of phosphate ester torsional conformations, Biochemistry 15 (1976) 3796–3803.
[5] D.G. Gorenstein, Nucleotide conformational analysis by ^{31}P nuclear magnetic resonance spectroscopy, Annu. Rev. Biophys. Bioeng. 10 (1981) 355–386.
[6] D.G. Gorenstein, Phosphorus-31 NMR: Principles and Applications, Academic Press, London, 1984.
[7] S. El antri, P. Bittoun, M.O.M. Monnot, O. Convert, E. Lescot, S. Fermandjian, Effect of distortions in the phosphate backbone conformation of six related octanucleotide duplexes on CD and ^{31}P NMR spectra, Biochemistry 32 (1993) 7079–7088.
[8] O. Mauffret, B. Hartmann, O. Convert, R. Lavery, S. Fermandjian, The fine structure of two DNA dodecamers containing cAMP responsive element sequence simulation studies, J. Mol. Biol. 227 (1992) 852–875.
[9] S. Schroeder, V.A. Roongta, J.M. Fu, C.R. Jones, D.G. Gorenstein, Sequence-dependent variations in the ^{31}P NMR spectra and backbone torsional angles of wild-type and mutant lac operator fragments, Biochemistry 28 (1989) 8292–8303.
[10] D.G. Gorenstein, B.A. Luxon, E.M. Glodfield, K. Lai, D. Vegeais, Phosphorus-31 Nuclear magnetic resonance of double- and triple-helical nucleic acids. Phosphorus-31 chemical shifts as a probe of phosphorus–oxygen ester bond torsional angles, Biochemistry 21 (1982) 580–589.
[11] V.A. Roongta, C.R. Jones, D.G. Gorenstein, Effect of distortions in the deozyribose phosphate backbone conformation of duplex

oligonucleotide dodecamers containing GT, GG, GA, AC, and GU base-pair mismatches on ^{31}P NMR spectra, Biochemistry 29 (1990) 5245–5258.
[12] C.A.G. Haasnoot, C. Altona, A conformational study of nucleic acid phosphate ester bonds using phosphorus-31 nuclear magnetic resonance, Nucleic Acids Res. 6 (1979) 1135–1149.
[13] D.G. Gorenstein, Stereoelectronic effects of biomolecules, Chem. Rev. 87 (1987) 1047–1077.
[14] D.G. Gorenstein, S.A. Schroeder, J.M. Fu, J.T. Metz, V. Roongta, C.R. Jones, Assignments of ^{31}P NMR resonances in oligodeoxyribonucleotides: origin of sequence-specific variations in the deoxyribose phosphate backbone conformation and the ^{31}P chemical shifts of double-helical nucleic acids, Biochemistry 27 (1988) 7223–7237.
[15] D.G. Gorenstein, Phosphorus-31 nuclear magnetic resonance of enzyme complexes: bound ligand structure, dynamics, and environment, Methods Enzymol. 177 (1989) 295–316.
[16] D.G. Gorenstein, Dependence of ^{31}P chemical shifts on O–P–O bond angles in phosphate esters, J. Am. Chem. Soc. 97 (1975) 898–900.
[17] C. Giessner-Prettre, B. Pullman, Quantum mechanical calculations of NMR chemical shifts in nucleic acids, Q. Rev. Biophys. 20 (1987) 113–172.
[18] D.B. Lerner, W.J. Becktel, R. Everett, M. Goodman, D.R. Kearns, Solvation effects on the ^{31}P-NMR chemical shifts and infrared spectra of phosphate diesters, Biopolymers 23 (1984) 2157–2172.
[19] A.J.R. Costello, T. Glonek, J.R. van Wazer, Phosphorus-31 chemical shift variations with counter cation and ionic strength for the various ethyl phosphates, Inorg. Chem. 15 (1976) 972–974.
[20] D.G. Gorenstein, E.M. Goldfield, R. Chen, K. Kovar, B.A. Luxon, High-resolution phosphorus nuclear magnetic resonance spectra of yeast phenylalanine transfer ribonucleic acid. Metal ion effects and tentative partial assignment of signals, Biochemistry 20 (1981) 2141–2150.
[21] K. Wüthrich, NMR of Proteins and Nucleic Acids, John Wiley and Sons, New York, 1986.
[22] S.L. Lam, L.N. Ip, X. Cui, C.N. Ho, Random coil proton chemical shifts of deoxyribonucleic acids, J. Biomol. NMR 24 (2002) 329–337.
[23] C.W. Kwok, C.N. Ho, L.M. Chi, S.L. Lam, Random coil carbon chemical shifts of deoxyribonucleic acids, J. Magn. Reson. 166 (2004) 11–18.
[24] D. Marion, K. Wüthrich, Application of phase sensitive two-dimensional correlated spectroscopy (COSY) for measurements of ^{1}H–^{1}H spin–spin coupling constants in proteins, Biochem. Biophys. Res. Commun. 113 (1983) 967–974.
[25] A.J. Shaka, K.J.R. Freeman, Evaluation of a new broadband decoupling sequence: WALTZ-16, J. Magn. Reson. 53 (1983) 313–340.
[26] A.J. Shaka, K.J.T. Frenkiel, R. Freeman, An improved sequence for broadband decoupling: WALTZ-16, J. Magn. Reson. 52 (1983) 335–338.
[27] A.J. Shaka, K.J. Broadband, spin decoupling in isotropic liquids, Prog. Nucl. Magn. Reson. Spectrosc. 19 (1987) 47–129.
[28] J.L. Markley, A. Bax, Y. Arata, C.W. Hilbers, R. Kaptein, B.D. Sykes, P.E. Wright, K. Wüthrich, Recommendations for the presentation of NMR structures of proteins and nucleic acids, J. Mol. Biol. 280 (1998) 933–952.
[29] K.E. Kover, V.J. Hruby, D. Uhrin, Sensitivity- and gradient-enhanced heteronuclear coupled/decoupled HSQC–TOCSY experiments for measuring long-range heteronuclear coupling constants, J. Magn. Reson. 129 (1997) 125–129.
[30] A.J. Shaka, C.J. Lee, A.J. Pines, Iterative schemes for bilinear operators: applications to spin decoupling, J. Magn. Reson. 77 (1988) 274–293.